



# EUROfusion

EUROFUSION WPJET1-PR(16) 15397

D Tegnered et al.

## **Gyrokinetic simulations of transport in pellet fuelled discharges at JET**

Preprint of Paper to be submitted for publication in  
43rd European Physical Society Conference on Plasma  
Physics (EPS)



This work has been carried out within the framework of the EUROfusion Consortium and has received funding from the Euratom research and training programme 2014-2018 under grant agreement No 633053. The views and opinions expressed herein do not necessarily reflect those of the European Commission.

This document is intended for publication in the open literature. It is made available on the clear understanding that it may not be further circulated and extracts or references may not be published prior to publication of the original when applicable, or without the consent of the Publications Officer, EUROfusion Programme Management Unit, Culham Science Centre, Abingdon, Oxon, OX14 3DB, UK or e-mail [Publications.Officer@euro-fusion.org](mailto:Publications.Officer@euro-fusion.org)

Enquiries about Copyright and reproduction should be addressed to the Publications Officer, EUROfusion Programme Management Unit, Culham Science Centre, Abingdon, Oxon, OX14 3DB, UK or e-mail [Publications.Officer@euro-fusion.org](mailto:Publications.Officer@euro-fusion.org)

The contents of this preprint and all other EUROfusion Preprints, Reports and Conference Papers are available to view online free at <http://www.euro-fusionscipub.org>. This site has full search facilities and e-mail alert options. In the JET specific papers the diagrams contained within the PDFs on this site are hyperlinked

# Gyrokinetic simulations of transport in pellet fuelled discharges at JET

D. Tegnered<sup>1</sup>, H. Nordman<sup>1</sup>, M. Oberparleiter<sup>1</sup>, P. Strand<sup>1</sup>, L. Garzotti<sup>2</sup>, I. Lupelli<sup>2</sup>,  
C. M. Roach<sup>2</sup>, M. Romanelli<sup>2</sup>, M. Valovič<sup>2</sup> and JET Contributors\*

EUROfusion Consortium, JET, Culham Science Centre, Abingdon, OX14 3DB, UK

<sup>1</sup> Chalmers University of Technology, SE-412 96 Gothenburg, Sweden.

<sup>2</sup> CCFE, Culham Science Centre, Abingdon, OX14 3DB, UK.

\* See the Appendix of F. Romanelli et al., Proceedings of the 25th IAEA Fusion Energy Conference 2014, Saint Petersburg, Russia

## Introduction

Pellet injection is the likely fuelling method of reactor grade plasmas. Injecting a pellet into the plasma temporarily perturbs both the density and temperature profiles, resulting in changes in dimensionless parameters such as  $a/L_n$ ,  $a/L_T$ , collisionality and plasma  $\beta$ . This will in turn affect microstability and transport properties of the discharge. Hydrogen pellet injection experiments were performed during the JET hydrogen campaign in 2014. The target were L-mode ICRH-heated hydrogen plasmas. The diagnostic set-up was optimised to measure the post pellet evolution of the density profile with high spatial resolution and the pellet injection frequency (14 Hz) was chosen with respect to sampling time of the Thomson scattering measurements (50 ms) to exploit a 'stroboscopic' effect and virtually enhance the time resolution of the profile measurement. Accurate equilibrium reconstruction and Gaussian process regression fits [1] of the kinetic profiles were performed to provide the basis for gyrokinetic analysis of the pellet cycle and characterise the transport properties of these pellet fuelled plasmas. The discharge under study here is no. 87847 with a toroidal magnetic field of 1.7 T, a plasma current of 1.75 MA and 3.45 MW of ICRH power. Microstability analysis of a typical MAST pellet fuelled discharge was previously performed in [2] where a stabilization of all modes in the negative  $a/L_n$  (positive density gradient) region was found.

The discharge is analysed at several radial positions around the density peak and at several time points after the injection of the pellet. The focus is on the time point when the density peak

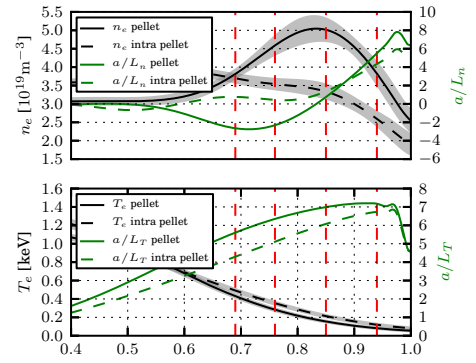


Figure 1: Profiles of density and temperature. Dashed lines indicate radial positions of the NL analysis.

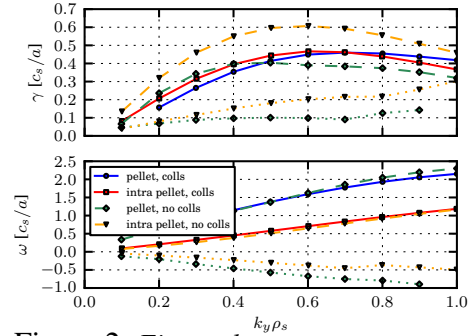


Figure 2: Eigenvalue spectra at  $\rho_{tor} = 0.69$ , subdominant modes dotted.

$\rho_{tor}$	$t$ [s after pellet]	$n$ [ $10^{19}/\text{m}^3$ ]	$T$ [keV]	$a/L_T$	$a/L_n$	$v_{ei}$ [ $c_s/a$ ]	$\beta$ [%]	$q$	$\hat{s}$
0.69	0.0042	3.81	0.43	5.60	-2.64	1.39	0.20	1.61	1.32
0.69	0.034	3.69	0.49	4.29	0.77	1.05	0.22	1.60	1.34
0.76	0.0042	4.59	0.28	6.35	-2.32	3.73	0.16	1.86	1.64
0.76	0.034	3.54	0.35	5.11	0.42	1.89	0.15	1.85	1.66
0.85	0.0042	5.01	0.15	7.00	0.74	13.00	0.10	2.30	2.20
0.85	0.034	3.34	0.21	6.08	1.36	4.74	0.09	2.30	2.22
0.94	0.0042	3.83	0.08	7.16	5.50	34.44	0.04	3.01	3.42
0.94	0.034	2.60	0.12	6.71	4.33	11.36	0.04	3.01	3.43

Table 1: Discharge parameters

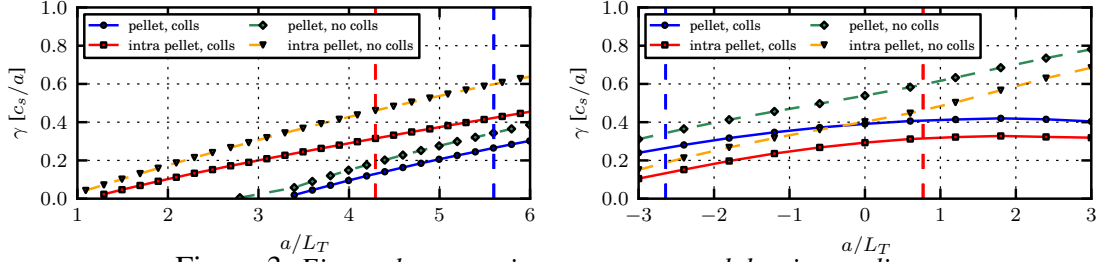


Figure 3: Eigenvalue scans in temperature and density gradients

35 from the ablation pellet is the largest,  $t = 0.0042$  s after the pellet injection, referred to as 'pellet'.  
36 The results are compared and contrasted to the time point when the peak is relaxed again at  
37  $0.034$  s, referred to as 'intra pellet'. The profiles of temperature and density and the resulting  
38 normalized gradient scale lengths are shown in Figure 1 and the discharge parameters are given  
39 in Table 1. Both linear and nonlinear simulations are performed in a flux tube domain using  
40 the gyrokinetic code GENE [3], including finite  $\beta$  effects and collisions in realistic geometry.  
41 We note that the collisionality is high in the present discharge and have included collisionless  
42 simulations in order to connect our results to more reactor relevant conditions.

### 43 GENE simulation setup and discharge parameters

44 GENE solves the nonlinear gyrokinetic Vlasov equation coupled with Maxwell's equations.  
45 Collisions are modelled using a linearised Landau-Boltzmann collision operator [4]. Magnetic  
46 fluctuations are included in all simulations. A numeric equilibrium reconstructed using the  
47 EFIT++ code [5] is used in a local, flux-tube domain.  $T_i = T_e$  and  $n_i = n_e$  is assumed, no  
48 impurities are included in the simulations. Fast particles and rotation are not expected to play an  
49 important role in this low- $\beta$ , ICRH heated discharge and are not included.

### 50 Linear results

51 Linearly the eigenvalue spectrum is dominated by the ITG mode for  $k_y \rho_s < 1.0$  and  $\rho_{tor} < 0.95$ .  
52 The eigenvalue spectra at the  $\rho_{tor} = 0.69$  position are shown in Figure 2 at the pellet and intra  
53 pellet time points. The pellet growth rates are slightly reduced in normalized units for  $k_y \rho_s < 0.7$   
54 in the collisional case while in the collisionless case the effect is more pronounced. In the

55 collisionless case there is a subdominant TE-mode which also has reduced growth rates at the  
 56 pellet time point.

57 In Figure 3 scans in temperature and density gra-  
 58 dients are shown at the pellet and intra pellet time  
 59 points, for  $k_y \rho_s = 0.3$  and  $\rho_{tor} = 0.69$ . However, the  
 60 results are general in the ITG wavenumber range  
 61 and in the negative  $a/L_n$  region. The pressure gra-  
 62 dient as considered in the curvature and  $\nabla B$  drifts  
 63 is calculated self-consistently from the density and  
 64 temperature gradients. In the  $a/L_T$  scan, the growth  
 65 rate is reduced in the pellet case at similar  $a/L_T$ ,  
 66 with a greater reduction in the collisionless case.  
 67 The ITG threshold is increased from  $a/L_T \sim 1$  in  
 68 the intra pellet case to  $a/L_T \sim 3$  in the pellet case.  
 69 In the  $a/L_n$  scan a reduction in growth rate is seen  
 70 in the collisional case both at high and low density  
 71 gradients. At similar  $a/L_n$  the pellet case is more  
 72 unstable because of the higher  $a/L_T$ . Taken together,  
 73 going from the intra pellet to the pellet case there is a stabilizing effect due to negative  $a/L_n$  but  
 74 a destabilizing effect due to an increase in  $a/L_T$  that partially undoes the stabilization, resulting  
 75 in the growth rate spectra exhibited in Figure 2.

## 76 Nonlinear results

77 For the nonlinear GENE simulations, a simulation domain in the perpendicular plane of 125  
 78 to 250 ion larmor radii in the poloidal direction and 110 to 240 in the radial direction was  
 79 typically used. with a typical resolution of  $[n_x, n_{k_y}, n_z, n_{v_{||}}, n_{\mu}] = [144, 48, 32, 64, 16]$ . The four  
 80 radial positions chosen for the nonlinear simulations are  $\rho_{tor} = 0.69$  and  $\rho_{tor} = 0.76$  in the  
 81 negative  $a/L_n$  region,  $\rho_{tor} = 0.85$  close to the peak of the pellet ablation profile and  $\rho_{tor} = 0.94$   
 82 in the positive  $a/L_n$  region. In order to make a more straightforward comparison between the  
 83 fluxes at different radial positions, the fluxes and resulting effective diffusion coefficients are  
 84 shown in SI units.

85 In Figure 4 the particle fluxes and diffusion coefficients at these radial positions are shown.  
 86 The particle flux is inwards on the inside of the pellet ablation peak and changes sign on the  
 87 outside. The particle fluxes are of similar magnitude but with different sign on each side of the  
 88 pellet ablation peak. In the negative  $a/L_n$  region the diffusion coefficients are lower just after

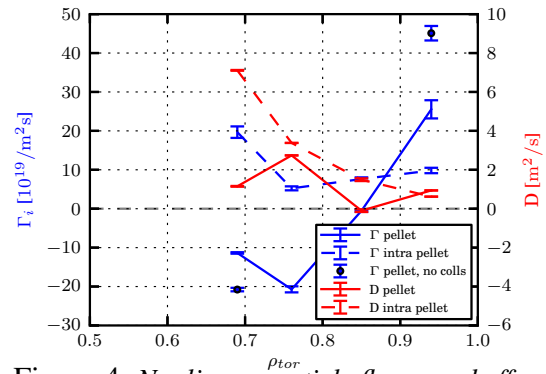


Figure 4: Nonlinear particle fluxes and effective diffusion coefficients.

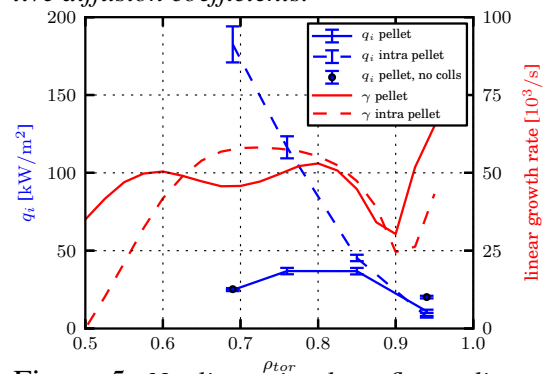


Figure 5: Nonlinear ion heat fluxes, linear growth rates at  $k_y \rho_s = 0.3$  also shown.

89 the pellet than at the intra-pellet time. The nonlinear ion heat fluxes are shown in Figure 5. The  
90 outward heat fluxes are greatly reduced in the negative  $a/L_n$  radial range compared to the intra  
91 pellet case. This, and the similar reduction in diffusion coefficients, is due to the reduction in  
92 nonnormalized growth rates, as displayed in the same figure. We have confirmed that the mean  
93 value and width of the ion heat flux spectra remain similar between the pellet and intra pellet  
94 cases. Collisionless simulations have also been performed at the  $\rho_{tor} = 0.69$  and  $\rho_{tor} = 0.94$   
95 radial positions of the pellet time point. They exhibit larger particle fluxes than the collisional  
96 case in with unchanged direction, as seen in Figure 4. A similar trend for negative  $a/L_n$  was  
97 found in [6].

## 98 Conclusions

99 In this paper transport analysis of a pellet fuelled L-mode JET discharge has been performed  
100 using the gyrokinetic code GENE. Linearly it was shown that the dominating ITG-mode was  
101 slightly stabilized in normalized units on the inside of the pellet ablation peak compared to  
102 the intra pellet interval when the density gradients had relaxed. While the negative  $a/L_n$  was  
103 stabilizing, this was partially counteracted by the increase in  $a/L_T$  on the inside of the pellet  
104 ablation peak compared to the intra pellet gradients, resulting in similar growth rates. Nonlinearly,  
105 the outward heat fluxes and diffusion coefficients were reduced on the inside of the peak compared  
106 to the intra pellet case. The particle fluxes on each side of the peak were of similar magnitudes  
107 but in different directions, suggesting a symmetric evolution of the post-pellet density profiles.  
108 Without collisions the particle fluxes were increased and remained in the same direction.

## 109 Acknowledgements and references

110 The simulations were performed on resources provided by the Swedish National Infrastructure for Computing  
111 (SNIC) at PDC Centre for High Performance Computing (PDC-HPC), on the HELIOS supercomputer system at  
112 Computational Simulation Centre of International Fusion Energy Research Centre (IFERC-CSC), Aomori, Japan,  
113 under the Broader Approach collaboration between Euratom and Japan, implemented by Fusion for Energy and  
114 JAEA. This work was funded by a grant from The Swedish Research Council (C0338001). This work has been  
115 carried out within the framework of the EUROfusion Consortium and has received funding from the Euratom  
116 research and training programme 2014-2018 under grant agreement No 633053. The views and opinions expressed  
117 herein do not necessarily reflect those of the European Commission.

## 118 References

- 119 [1] MA Chilenski, M Greenwald, Y Marzouk, NT Howard, AE White, JE Rice, and JR Walk. *Nuclear Fusion*,  
120 55(2):023012, 2015.
- 121 [2] L Garzotti, J Figueiredo, CM Roach, M Valovič, D Dickinson, G Naylor, M Romanelli, R Scannell, G Szepesi,  
122 MAST Team, et al. *Plasma Physics and Controlled Fusion*, 56(3):035004, 2014.
- 123 [3] <http://genecode.org/>.
- 124 [4] F Merz. *Gyrokinetic simulation of multimode plasma turbulence*. PhD thesis, Universität Münster, 2008.
- 125 [5] LC Appel, GTA Huysmans, LL Lao, PJ McCarthy, DG Muir, ER Solano, J Storrs, D Taylor, W Zwingmann,  
126 et al. A unified approach to equilibrium reconstruction. In *Proceedings-33rd EPS conference on Controlled  
127 Fusion and Plasma Physics*, pp. P-2.160, 2006.
- 128 [6] B Baiocchi, C Bourdelle, C Angioni, F Imbeaux, A Loarte, M Maslov, and JET Contributors. *Nuclear Fusion*,  
129 55(12):123001, 2015.